Journal of Computational and Applied Mechanics, Vol. 6., No. 1., (2005), pp. 39–52

SHAPE FINDING OF AN EXTREMELY TWISTED RING

Zsolt Gáspár[1,2], Robert Németh[1,3]
[1]Department of Structural Mechanics
[2]HAS Research Group for Computational Structural Mechanics
[3]Center for Applied Mathematics and Computational Physics
Budapest University of Technology and Economics
H-1521 Budapest, Műegyetem rkp. 3., Hungary
`gaspar@ep-mech.me.bme.hu, nemeth.robert@gmx.net`

[Received: June 2, 2004]

Abstract. The Kirchhoff rod is a widely used model in describing configurations of DNA chains. In the simplest case of such research the molecule-chain is represented by a twisted-bent rod. In this paper we will present an application of this rod model for describing the shapes of the DNA chain in a special configuration. Here, two finite segments of the rod are in contact with each other. The contact region is closed on each end by terminal loops. These configurations can be represented by four parameters. The equilibrium path is computed in the four-dimensional space of the parameters using the path-following simplex method. The paper shows the system of equations applied during the path-following, equilibrium path from a generalized solution, and some numerical results with different rod lengths. At last we show how our results should be connected to configurations of former research.

Mathematical Subject Classification: 70G45
Keywords: twisted ring, large displacements, DNA

1. **Introduction**

Let us consider an initially straight rod a with circular cross-section of radius r. The rod is long, i.e. $L >> r$, where L is the length of the rod. The rod is made of a homogenous, linearly elastic material with the modulus of elasticity E and the shear modulus of elasticity G. Bending stiffness is characterized by the constant $A = EI_x$, where $I_x = \frac{r^4\pi}{4}$, and the twist stiffness by $C = GI_p$, where $I_p = \frac{r^4\pi}{2}$. The rod is supposed to be inextensible and unshearable. First, the rod is bent to a ring with a pair of moments acting on the end-sections. Then the end-sections are twisted in the opposite direction, while they stay in contact. By a small twist rate the ring holds its planar shape. Above a critical value of twist, the ring loses its stability, and the rod takes a spatial shape. The critical value of twist rate was first estimated by Zajac [1]. Dichmann et al. [2] presents critical values even for overlapping rings. Another, symmetry-based examination of all configurations of self-penetrable rods was presented by Domokos [3]. If the rod is impenetrable, self-contact can arise. The contact may destroy some symmetry properties of the solutions. The self-contact can arise in contact points, or along a contact-line. Coleman et al. [4] determined equilibrium paths of the rod with self-contact, with detailed analysis of the stability of solutions. In addition to the classification of different contact configurations, Swigon et al. [5] derived the differential equation of the generalized helix, which occurs in the case of self-contact along a line, and its analytical solution. An extension of their work was made by Thompson et al. [6], where the generalized helix is loaded by a wrench.

In the above mentioned research the elastic rod is treated as a continuous mechanical model of DNA molecules, where the rod axis is equivalent to the duplex axis of the DNA. This modelling is validated through similarity between computed rod shapes and real DNA configurations taken from electron-microscope photos.

In this paper we want to give an extension to the former results. The first configuration on the first non-trivial equilibrium path of the impenetrable rod has one point of contact. In a contact point a concentrated contact force arises. This configuration is denoted by A_1, where A means the first non-trivial path, while 1 is the number of contact point(s). The following shapes on this path have 2 and 3 contact points, these are denoted by A_2 and A_3. Further increasing of the twist leads to the A_4 configuration. The A_4 configuration differs from the previous configurations in a contact line between the inner contact points. In the contact line a distributed contact force arises. However, a contact line contains an infinite number of contact points. We refer to a point as a contact point only if there a concentrated (finite) force arises. Further increasing of the twist rate leads to a longer contact line, while the free segment between the outer and inner contact points decreases, so does the length of the terminal loop. We suspect that at extreme high twist the free segment disappears. Then we will have a configuration with two contact points, but, unlike the A_2 configuration, there will be a contact line between the contact points. So, we will refer to this configuration as A_{2+}. Our goal is to find the equilibrium path of this configuration. We do not deal with the stability of the solutions.

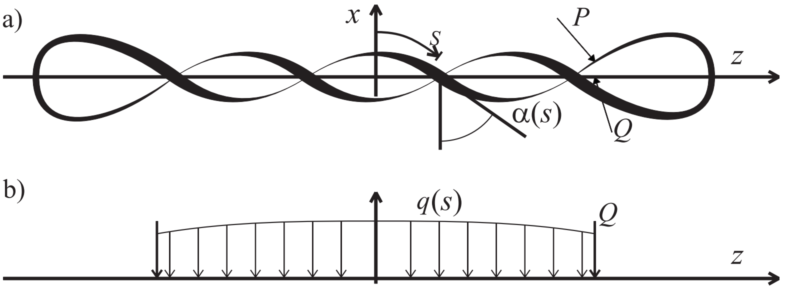

Figure 1. (a) Sketch of the analyzed configuration with the global reference system. (b) Intensity of the assumed distributed ($q(s)$) and concentrated (Q) contact forces along the contact line

The axis of an A_{2+} configuration is sketched in the Figure 1a. The configuration is symmetric to the contact line, we refer to this axis by z. We set its 0 to the middle of the contact line. So, the rod axis crosses the plane $z = 0$ in two points. Through these points goes axis x, which is also an axis of symmetry. The third axis of our reference system will be axis y. The coordinate system $[xyz]$ is a right-handed one, therefore axis y points out of the plane in Figure 1a.

Every configuration can be represented by the space curve of the rod axis. This curve will be given by the co-ordinates in the system $[xyz]$, as a function of the arc length s. The point $s = 0$ should be where the rod axis crosses the plane $z = 0$ at a positive value of x. The rod is directed in such a way that a small increase in the arc-length parameter leads to a point in the positive eighth of the reference system. (This happens if we twist the rod in clockwise direction.) In the contact region the rod axis describes a generalized helix. The rise angle $(\alpha(s))$ of this helix depends on s, and is defined as the angle between the tangent of the rod axis and a plane normal to z. In the examined configuration it is sufficient to examine the segment from $s = 0$ to $s = L/4$. The last point is the top of the closing loop on the right side.

We divide the examined part of the A_{2+} configuration into two different parts. The first is the helix, where the rod is in contact with another part of the rod. On the contact line arises the distributed contact force $q(s)$, which points from axis z to the rod axis. The last cross-section of contact is at the arc-length s_P. The second part is the terminal loop. In the loop there are no external forces acting on the rod. At the common boundary of these two parts a concentrated contact force (Q) arises (Figure 1b.).

In Section 2 we will show the differential equations used for finding a rod shape, then, in Section 3 we will present the equation system to be solved for the equilibrium path. In Section 4 the applied numerical methods of computation will be introduced. Numerical results and their conclusions will be presented in Section 5.

2. Differential equations applied

2.1. Differential equation of the generalized helix.

The differential equation of the generalized helix is derived from the geometrical, equilibrium and constitutive equations of the rod. The whole derivation can be found in [5], [6] and [7], interested readers are directed to those works. Here we only present the start-up and the definitions of the terms used.

The turn of the rod around the contact line is measured through the function $\varphi(s)$, as it is shown in Figure 2a. So the co-ordinates of the rod axis at the arc-length s are:

$$\mathbf{r}(s) = \begin{bmatrix} r \cdot \cos\varphi(s) \\ r \cdot \sin\varphi(s) \\ z(s) \end{bmatrix}.$$

Figure 2b helps us to write the first and second derivatives of $\mathbf{r}(s)$. The length of the latter is the curvature of the curve.

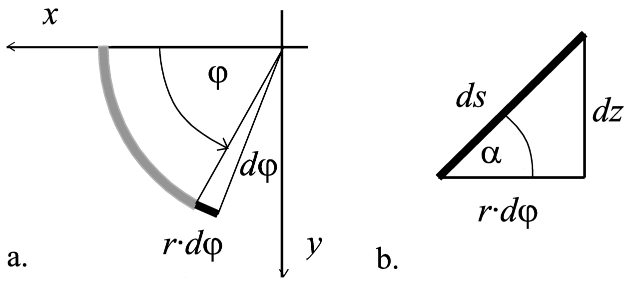

Figure 2. Geometry of generalized helix. View of an elementary segment (a) from axis z (b) from a radial direction

The simplest way of writing the six differential equations of equilibrium is to use a cylindrical reference system. We have only three equations of material behavior, because the effect of normal and shear forces is neglected. The first one is the relationship between the twist ω and the torque M_T:

$$\omega = \frac{M_T}{C}, \tag{2.1}$$

the second one describes the relationship between the curvature κ and the bending moment M_B

$$\kappa = \frac{M_B}{A}, \tag{2.2}$$

and the third one states that the moment vector $\mathbf{M}$ is orthogonal to the principal normal vector $\mathbf{r}''$:

$$\mathbf{M} \cdot \mathbf{r}'' = 0, \tag{2.3}$$

where $'$ denotes differentiation with respect to s.

From these equations one can derive the differential equation of the generalized helix:

$$0 = \alpha''' + \alpha' \frac{2r^2\alpha'' \sin 2\alpha + 8\cos^6\alpha - 12\cos^4\alpha + 6\cos^2\alpha}{r^2\cos 2\alpha}. \tag{2.4}$$

This differential equation can be written in a second order form, where the constant torque appears as a free parameter:

$$\alpha'' = \frac{M_T \cdot \cos 2\alpha}{A \cdot r} - \frac{\sin 2\alpha \cdot \cos^2\alpha}{r^2}. \tag{2.5}$$

2.2. **System of differential equations of a free segment.** In the case of a free segment the first step of the computation of the shape (namely the function $\mathbf{r}(s)$) is to compute the inner forces and moments. There are no external forces acting on the rod, so the equilibria of a segment of arbitrary length causes the resultant of the inner forces to be constant along the segment. This resultant will be reduced to the origin of the reference system, and the force and moment components will be denoted by vectors $\mathbf{P}_0$ and $\mathbf{M}_0$. The effect of normal and shear forces is neglected, so we need the moments in the cross-sections only. Their vector can be computed by the form:

$$\mathbf{M}(s) = \mathbf{M}_0 + \mathbf{P}_0 \times \mathbf{r}(s). \tag{2.6}$$

It is a well-known fact that the torque and the specific twist are constant in the initially straight rod of homogenous cross-section. So the twist of a segment can be computed from the specific twist and the length. The bending part of the moment vector causes a change in the tangent of the rod, which can be computed from:

$$\mathbf{r}''(s) = \frac{1}{A}\mathbf{M}(s) \times \mathbf{r}'(s). \tag{2.7}$$

3. Closing conditions of rod

3.1. **Equation system of closing.** We use the symmetry of the rod in our computation, so we examine only a quarter of the whole rod. The shape of a rod can be specified by four parameters. Three of these parameters are connected to the helix, the fourth parameter belongs to the contact point. In the point $s = 0$ the initial value of the rise angle (α_0) and its first and second derivatives ($\alpha_0^{'}$ and $\alpha_0^{''}$) determine the shape of the helix. The symmetry causes $\alpha_0^{'} = 0$, so here we have only α_0 and $\alpha_0^{''}$ as free initial values. The third parameter of the helix is its length, denoted by s_P. The fourth parameter is the concentrated contact force Q at the end of the helix. The function of the inner forces in the helix can be computed from the three parameters α_0, $\alpha_0^{''}$ and s_P, their radial force component is modified at the end point by Q.

Any set of the above parameters allows the computation of a rod shape. First the helix-form must be computed as an initial value problem from $s = 0$ up to $s = s_P$. Then the radial component of the inner forces must be modified by Q, and the system of differential equations of the closing loop must be solved until $s = L/4$. The parameters lead to a closed rod, if this point is the top of the loop, namely the rod crosses axis z in this point orthogonally. This can be mathematically formulated with three equations: $x(L/4) = 0$, $y(L/4) = 0$ and $z^{'}(L/4) = 0$.

(Note: The helix has a third-order differential equation, so the whole helix can be defined by four values, the length of the helix and three initial values. The same helix could be defined by other values, for example by the length, the rise angle in the end points, and the first derivative in the start-point. Naturally, the latter must be equal to zero, as before.)

3.2. **Possible shapes.** On the basis of the previous subsection, four parameters define a rod shape. We call this rod shape a mathematically possible solution, if the three equations for closing are satisfied.

Physically acceptable solutions are those mathematically possible solutions for which the following conditions are fulfilled:

- the rod does not cross itself,
- no tension arises in contacts.

The first condition is satisfied, if the largest curvature is smaller than the reciprocate of the radius of the rod, and the rise angle of the helix causes no self-intersection (which in [8] occurs at $\alpha = 45°$). The second condition means, that Q and the minima of q cannot be negative.

4. **Numerical method of solution**

The first step of the solution is to find the mathematically possible shapes, then the physically unacceptable solutions will be filtered out. The units of lengths and forces are chosen to have $r = 1$ and $A = 1$.

4.1. **The Path-Following Simplex Algorithm.**

In order to determine the mathematically possible shapes, we have to find the common zero places of $n - 1 = 3$ functions, depending on $n = 4$ parameters. The number of functions and parameters suggests that the solution set is a one dimensional set in the space of parameters. This type of problems can be easily solved by the Path-Following Simplex Algorithm [9]. We set a simplex in the space of the parameters with one side over a known solution. Then we compute the values of the error-functions (the left sides of the closing equations, i.e. $x(L/4)$, $y(L/4)$ and $z^{'}(L/4)$) in the vertices of the simplex and interpolate them. So, each function will have a solution set of $n - 1$ dimensional hyperplane. The common crossing line of these planes will be a line. This way we linearize the solution. The linearization gives a good approximation of the solution inside the simplex. The linearized solution crosses two simplex sides. One side is where the known result lies, the other one is a new solution point. We mirror the simplex on this side, then we have a new simplex with a solution on one of its sides. Now we can linearize the solution inside this simplex, just as we did with the previous one, but now we have to compute the error-functions in only one vertex, because the mirroring does not change the position of the mirroring side. The persistent use of the above steps leads to a whole solution (or, at least its good approximation by a piecewise linear curve).

The path following requires a starting point. Domokos and Szeberényi [10] present a method, where the path following is combined with scanning the parameter space. We can also fix the value of one parameter, then, an iterative method provides one solution point of the equation system. The drawback of this method is that a change in the length of the rod causes change in the initial solution.

A different reading of parameters can result an universal solution point. If the rise angle of the helix is constant (providing $\alpha_0 = \alpha_P$), then the internal forces and moments are also constant. So they do not depend on the length of the helix, and the terminal loop is also independent of L. In other words, the value of s_P changes, but $L/4 - s_P$ remains unattended. So we have to compute the free segment of length $L/4 - s_P$ connecting to a helix of constant rise angle α_0 with the inner forces determined by the helix and the modifier contact force Q. The three variables mentioned above have to be computed according to the connecting equations.

The problem can be solved even with two unknown parameters only, if we compute the free segment until the third equation, namely $z^{'}(L/4) = 0$ comes true. Then we only have to solve the equation system $x = 0$, $y = 0$ for the variables α_0 and Q, while $L/4 - s_P$ will be the arc-length, belonging to the solution. The result of this computation is:

$$\alpha_0 = 0.9733982, \qquad L/4 - s_P = 3.5773973, \qquad Q = 0.3212820.$$

These data determine the starting point of the path following. But this starting point is only a mathematically possible solution, because on the top of the loop the rod would have too high a curvature. This would lead to an overlap at the top of the loop, as can be seen in Figure 3.

Figure 3. The physically non-acceptable terminal loop at universal starting point

4.2. **Finite differences of variable length.**

4.2.1. *Reason of using FDVL.* The generalized helix has a third-order differential equation. In order to compute the error-functions of the simplex path-following, one has to solve this differential equation. The analytical solution of the differential equation is given in the paper by Coleman et al. [11]. This solution contains elliptic integrals, and has singularity at our desired starting point and is numerically instable in its neighborhood. That is the reason why we choose a numerical method for solving the boundary value problem of the helix. The helix is then determined through its length s_p, its rise angles in start and end-points (α_0, α_P) and the first derivatives of the rise angle (which is equal to 0). The differential equation can be transformed into a first-order form:

$$(\alpha^{'})^2 = \frac{M_T \cdot \sin 2\alpha}{A \cdot r} + \frac{\cos^4 \alpha}{r^2} - \frac{M_T \cdot \sin 2\alpha_0}{A \cdot r} - \frac{\cos^4 \alpha_0}{r^2}. \tag{4.1}$$

This form contains M_T as an unknown parameter, and satisfies the $\alpha_0^{'} = 0$ condition. From the analytical solution of the helix one can show, that the function $\alpha(s)$ changes monotonous in the interval $[0, s_P]$, so the sign of the first derivatives equals to the difference of $\alpha_P - \alpha_0$. The function does not leave the interval of α_0 and α_P, as another consequence of monotony.

4.2.2. *Computational form of the finite differences.* We divide the interval $s = [0, s_p]$ into N_d sections. The length of the ith section is denoted by Δs_i. The analytic solution shows that the function changes less at small s; a sketch of the function can be found in the paper by Thompson et al. [6]. It is preferable to choose the sections so that the changees of the function over the sections are approximately the same in size. This condition needs longer sections at smaller changes of function and shorter sections at greater changes of function. Let the lengths of sections Δs_i make a geometrical series. The quotient of two consecutive sections' length $\Delta s_{i+1}/\Delta s_i$ is denoted by $q \leq 1$, so the last (the N_dth) section's length is $\Omega = q^{(N_d-1)}$ times the first section's length. So the sum of all sections, i.e. the length of the helix is:

$$s_P = \Sigma_{i=1}^{N_d} \Delta s_i = \Delta s_1 \cdot \Sigma_{i=1}^{N_d} q^{i-1},$$

while the length of first section (Δs_1) is:

$$\Delta s_1 = s_p \cdot \frac{1-q}{1-q^{N_d}} .$$

We want to compute the function values α_i in the end-points of the sections. (This notation leaves α_0 unchanged, as a continuation of the series, while at the end of the helix $\alpha_{N_d} = \alpha_P$.) There are $N_d - 1$ unknown α_i values in the divider points, and we do not know M_T yet. One can write $N_d - 1$ equations with the finite differences (one for each divider point), and one more for the start-point of the helix, using the symmetry of function $\alpha(s)$.

We write the difference equation of the ith divider point. The truncated Taylor-series of α at that point is:

$$\alpha(s_i + S) = \alpha_i + \alpha_i^{'} \cdot S + \alpha_i^{''} \cdot \frac{S^2}{2},$$

so we can write α_{i-1} and α_{i+1}:

$$\alpha_{i-1} = \alpha_i - \alpha_i^{'} \cdot \Delta s_i + \alpha_i^{''} \cdot \frac{\Delta s_i^2}{2},$$

$$\alpha_{i+1} = \alpha_i + \alpha_i^{'} \cdot \Delta s_i \cdot q + \alpha_i^{''} \cdot \frac{\Delta s_i^2}{2} \cdot q^2.$$

These lead to the following expression for α''_i:

$$\alpha_i'' = \frac{2}{q \cdot (q+1) \cdot \Delta s_i^2} \left(q \cdot \alpha_{i-1} - (q+1) \cdot \alpha_i + \alpha_{i+1}\right),$$

which must be equal to the formula given by (2.5), i.e.

$$M_T \cdot \cos 2\alpha_i - \sin 2\alpha_i \cdot \cos^2 \alpha_i = \tag{4.2}$$

$$= \frac{2}{q \cdot (q+1) \cdot \Delta s_i^2} \cdot (q \cdot \alpha_{i-1} - (q+1) \cdot \alpha_i + \alpha_{i+1}) \ . \tag{4.3}$$

This equation can be written for $N_d - 1$ points. In the ‘zeroth’ point a fictitious -1st point helps to write the following equation:

$$M_T \cdot \cos 2\alpha_0 - \sin 2\alpha_0 \cdot \cos^2 \alpha_0 = \frac{2}{\Delta s_1^2} \cdot (\alpha_1 - \alpha_0). \tag{4.4}$$

The helix is computed by the solution of equations (4.2) and (4.4). The N_d equations are solved with an iterative method.

4.2.3. *Iterative solution of the equation system of finite differences.* The function values in the divider points can be set initially in order to make a second order parabola. Initial values of α_i-s will be

$$\alpha_i = \alpha_0 + \left(\frac{\Sigma_{j=1}^{i} \Delta s_j}{s_p} \right)^2 (\alpha_P - \alpha_0),$$

and the initial value of M_T is computed from Eq. (4.4). In every iteration step we change

- α_i-s by the formula

$$\alpha_i^{new} = \frac{q \cdot \alpha_{i-1} + \alpha_{i+1}}{q+1} - (M_T \cdot \cos 2\alpha_i - \sin 2\alpha_i \cdot \cos 2\alpha_i) \cdot \frac{q \cdot \Delta s_i^2}{2}, \tag{4.5}$$

  $i = 1, ..., N_{d-1}$, which was expressed from Eq. (4.2) (where on the right side we use the modified value of α_{i-1}, but the old values of α_i and α_{i+1}),
- M_T from Eq. (4.4).

If the greatest change of α_i-s is smaller than a prescribed limit $\Delta\alpha$, we stop the iteration.

$\alpha^{'}(s)$, $\alpha^{''}(s)$ and the internal forces can be computed at the end-point of the helix from the accepted values of α_i-s.

5. **Numerical results**

5.1. **Equilibrium paths and configurations.** We choose the length of the rod to $L = 244$, and $C = 2/3$, in order to reach comparable results with previous results in [4]. The helix was divided into 250 sections, the quotient of the largest and smallest section was 30, i.e. $q = 30^{-1/249} \approx 0.9864334$. Figure 4. shows two dimensional projections of the mathematically possible solutions. On the upper vertical axes the rise angles are in the middle of the helix, on the lower axes are the lengths of the half-loop. The horizontal axes represent the rise angle at the end-point of the helix on the left side, and the contact force on the right side.

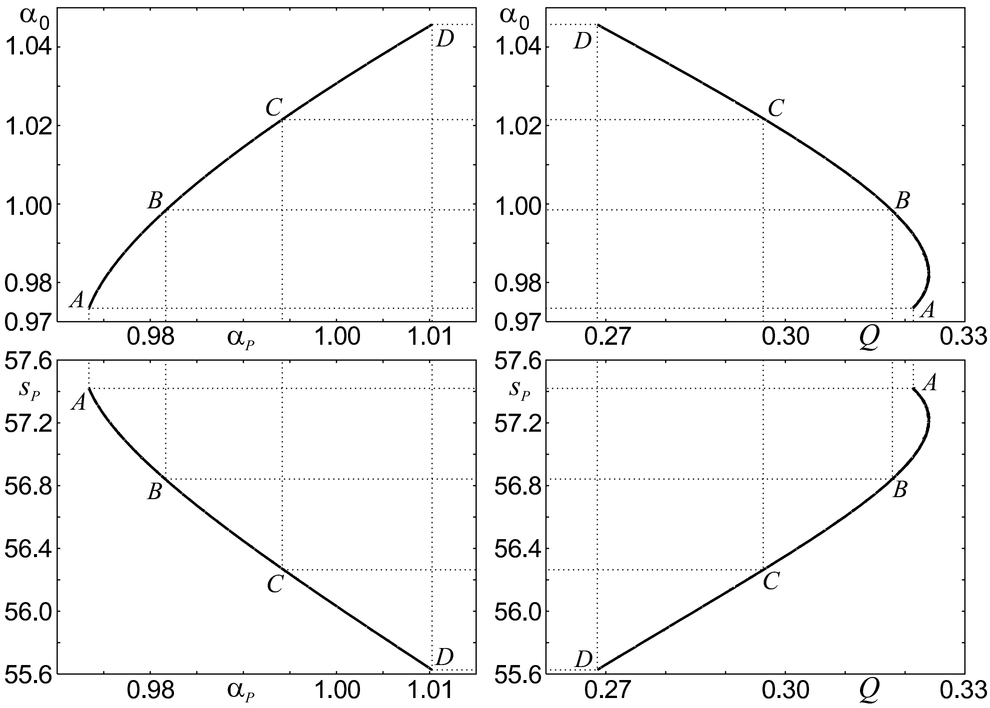

Figure 4. Two dimensional projections of the equilibrium path of the rod with $A = 1$, $L = 244r$.

We mark four points in each diagram. Point A is the starting point of the path following procedure. The smallest curvature is 1 in point B, and the minimum of the distributed contact force is 0 in point D. Physically acceptable shapes belongs to points of segment BD. One example for that is point C.

Figure 5a-d represents four rod shapes from the equilibrium path, namely the configurations in points A, B, C and D, respectively. The series of the presented shapes can be reached through an unloading process during which the twist rate decreases from B to D. (It decreases even from A, but those are physically non-acceptable solutions, hence they are out of our interest.) But the smaller twists are still very high, as the following short computation will show.

We calculate the characteristic values of the space curve of the configuration of Figure 5c. In this configuration the torque equals $M_T = -0.533444$, the rise angle of the helix in its mid-point is $\alpha_0 = 1.021554$ and the arc-length of the helix is $s_P = 56.269746$. The characteristic values are the twist (Tw), the writhe (Wr) and the link (Lk). Their meanings for a space curve and a rod can be found in the works by White [12] and Fuller [13]. The twist can be computed from the torque, and, as

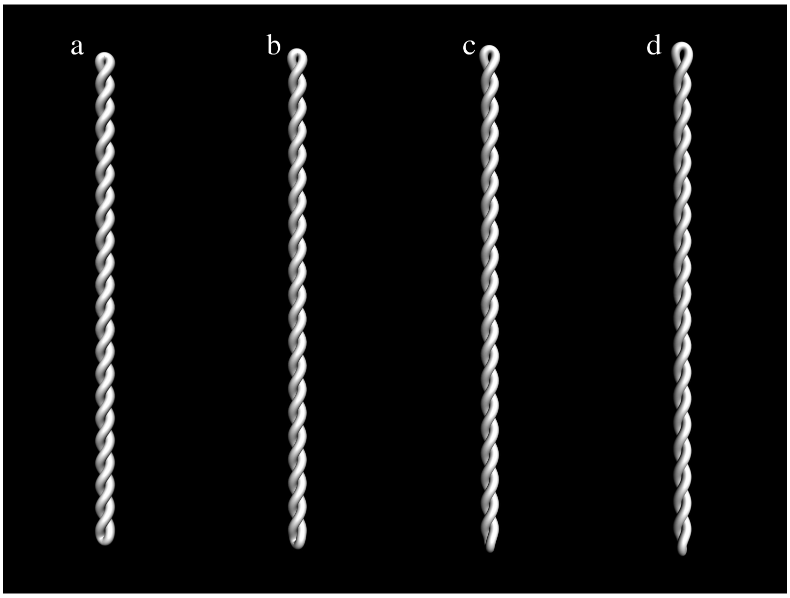

Figure 5. Equilibrium shapes of the rod, corresponding to the points A, B, C, D of the eq. path

already mentioned, it is constant along the rod, so it can be computed via

$$Tw = \frac{M_T}{C}\frac{L}{2\pi} \; . \tag{5.1}$$

C depends on the material of the rod, and until now it has not had any influence on the computation. The earlier mentioned C results $Tw = -31.08$.

The writhe is computed with an approximate method presented by Thompson et al. in [6]. We assume that the bulk of writhe is in the helix, and neglect the writhe that would be computed from the loop. We can also neglect the small change of the rise angle, so we compute the writhe on a helix of constant rise angle α_0 via:

$$Wr = \frac{2s_P \cos^2 \alpha_0}{\pi} = -9.77 \; . \tag{5.2}$$

The link number is the measure of the twist of the end sections against each other:

$$Lk = Tw + Wr = -40.85 \; . \tag{5.3}$$

Comparing these results with the graphs of Coleman et al. in [11] one can prove the intuition that our analyzed shapes arise at a very high twist.

5.2. **Connection to former results.** The characteristic values of the configuration D can be computed in the same way, as we did in the previous subsection. Then we had the link number $Lk = -34.05$. In this configuration the minimum of distributed contact force equals zero. Further decreasing of the twist results in the need

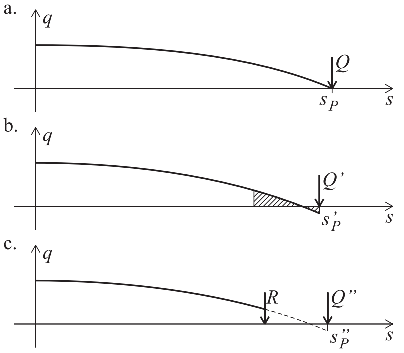

Figure 6. Change of distributed contact forces (a) in D state, (b) in a physically non-acceptable state after decreasing the twist, (c) in a possible new configuration (A_4)

of tensional forces between the strands of the helix. Since this is not a physically acceptable configuration, no A_{2+} configuration exists with a lower link number than configuration D.

We present some theoretical considerations on what kind of configuration may arise if we decrease the twist in state D. The twist of the end-sections against each other is measured with the link number. Decreasing the twist means decreasing the link, i.e. the rod has to change to a new configuration, but this new configuration has nearly the same link number.

The character of the intensity of the distributed contact force is sketched on Figure 6. Configuration D with vanishing contact force at its end is in Figure 6a., while Figure 6b. shows the necessary distribution, when the twist is decreased and we use the same equations. In physically acceptable solutions no negative contact force arises, so a part of the rod will shove off its contacting part. We suspect that the contact ends in the hatched region, and at the end of the remaining contact a second concentrated force arises instead of the contact forces of the hatched region. This force is denoted by R in Figure 6c. That means that the follower configuration in the un-twisting process could have a line contact, closed by the concentrated contact force R, then a skip-fly segment, followed by the force Q'', then it is closed by the terminal loop. In short, this will be an A_4 configuration with link number -34.05.

As we presented the analyzed A_{2+} configuration arises only at very high twist values. In this state a secondary buckled shape is also possible. In the resulting configuration the double helix wraps around itself. This would be the third helical form, as the rod itself is the model of the double-helix of the DNA, it creates the generalized helix we have presented, and the generalized helix produces a more complex helix with a very complicated contact situation.

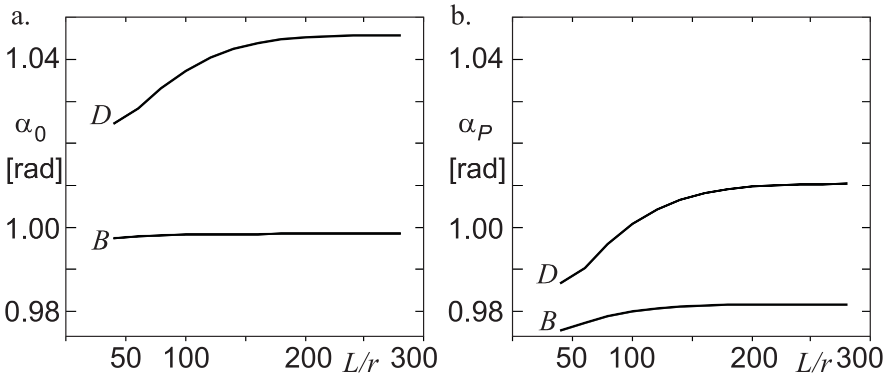

Figure 7. The rise angle in the middle (a) and at the end (b) of the helix in terms of the function of rod length. The upper and lower linse represent states D and B, respectively.

5.3. **Effect of change in the rod length.** We analyzed the effect of rod length. Figure 7 shows two graphs of results. Both graphs present a change of the rise angle as a function of the rod length, Figure 7a at the middle of helix, while Figure 7b at the end. The physically unacceptable universal starting point of path following has a constant value of 0.9733982. From there all angles are increasing until state B, which is the lower graph in both figures. The maximum of attainable angles arises in state D, which are shown by the upper lines.

The rod length was changed between 40 and 280. It can be seen that the interval of physically acceptable states increases with increasing rod length. We can see from the graphs that for long rods the angles vary only by a small value and it seems that all four curves have a horizontal asymptote. This is valid for relatively long rods, where the twisted part is long enough to result in very small derivatives even in case of larger difference between the rise angle in the middle and at the end of the helix. Moreover, the longer the rod is, the longer part of it lies in the helix, in accordance with the assumption made by the approximate computation of the writhe.

In the case $L = 4 \cdot 3.5773973 = 14.3095892$ the length of the contact line would be equal to 0. The un-twisting process should decrease this length, but it cannot be negative, so this is a theoretical lower end of the diagrams. This configuration could also be treated as an A_1 configuration of a short rod. However, this configuration is physically non-acceptable, as its curvature is greater than $1/r$; an unloading process of the rod can reach possible shapes of the rod, but this is beyond the scope of this paper.

5.4. **Conclusions.** We presented the numerical computation of a twisted elastic ring in a configuration with self-contact along a line, where no skip-fly segment arises between the contact line and the terminal loop. The equilibrium path of the rod shape was computed with the Path-Following Simplex Algorithm in the space of the parameters defining the rod shape. An universal starting point, independent of the rod length was given to the path-following. Using an approximate method for computing the twist and writhe of the spatial curve, we proved that the assumed configuration arises at very high twist rates beyond the interests of former research work.

Acknowledgement. The authors gratefully acknowledge the useful discussions with G. Domokos and the support of the Hungarian Grants FKFP-0177/2001 and OTKA-T37880.

REFERENCES

1. Zajac, E. E.: Stability of two planar loop elasticas. *J. Appl. Mech.*, **29**, (1962), 136-142.
2. Dichmann, D. J., Li, Y. and Maddocks, J. H.: Hamiltonian formulations and symmetries in rod mechanics. In: J. P. Mesirov, K. Schulten, D. W. Sumners, eds., *Mathematical Approaches to Biomolecular Structure and Dynamics*, Springer, New York, 1996, 71-113.
3. Domokos, G.: A group theoretic approach to the geometry of elastic rings. *J. Nonlinear Science*, **5**, (1995), 453-478.
4. Coleman, B. D., Swigon, D. and Tobias, I.: Elastic stability of DNA configurations. II. Supercoiled plasmids with self-contact. *Physical Review E*, **61**, (2000), 759-770.
5. Swigon, D., Coleman, B. D. and Tobias, I.: The elastic rod model for DNA and its application to the tertiary structure of DNA minicircles and mononucleosonmes. *Biophysical Journal*, **74**, (1998), 2515-2530.
6. Thompson, J. M. T., van der Heijden G. H. M. and Neukirch, S.: Super-Coiling of DNA-Plasmids: the Generalised Ply. *Proc. R. Soc. Lond., Series A*, **458**, (2002), 959-985.
7. Gáspár, Z. and Németh, R.: A special shape of a twisted ring. *Proc. of 2nd European Conference on Computational Mechanics*, CD p. 11, 2001.
8. Przybyl, S. and Pieranski, P.: In search of ideal knots III Application of Maple V.4 to the problem of two ropes tightly twisted together. *Pro Dialog*, **6**, (1998), 18. (in Polish)
9. Domokos, G. and Gáspár, Z. A global, direct algorithm for path-following and active static control of elastic bar structures. *Int. J. of Structures and Machines*, **23**, (1995), 549-571.
10. Domokos, G. and Szeberényi, I.: A hybrid parallel approach to nonlinear boundary value problem. *Computer Assisted Mechanics and Engineering Sciences*, **11**, (2004), 15-34.
11. Coleman, B. D. and Swigon, D.: Theory of supercoiled elastic rings with self-contact and its application to DNA plasmids. *J. Elasticity*, **60**: (2000), 173-221.
12. White, J. H.: Self-linking and the Gauss integral in higher dimensions. *Am. J. Math.*, **91**, (1969), 693-728.
13. Fuller, F. B.: The writhing number of a space curve. *Proc. Natl. Acad. Sci. USA.*, **68**, (1971), 815-819.